Polymer Testing 116 (2022) 107807

Contents lists available at ScienceDirect

Polymer Testing

journal homepage: www.elsevier.com/locate/polytest

Analysis of the influence of microencapsulated phase change materials on the behavior of a new generation of thermo-regulating shape memory polyurethane fibers

José Manuel Laza [a,*], Antonio Veloso-Fernández [a], Julia Sanchez-Bodon [a], Ane Martín [a], Amaia M. Goitandia [b], Cristina Monteserín [b], Xabier Mendibil [b], Karmele Vidal [b], Jon Lambarri [b], Estibaliz Aranzabe [b], Miren Blanco [b], José Luis Vilas-Vilela [a,c]

[a] Grupo de Química Macromolecular (LABQUIMAC), Departamento de Química Física, Facultad de Ciencia y Tecnología, Universidad del País Vasco UPV/EHU, 48940, Leioa, Spain
[b] Unidad de Química de superficies y Nanotecnología, Fundación Tekniker, Iñaki Goenaga 5, 20600, Eibar, Spain
[c] BCMaterials, Basque Center for Materials, Applications and Nanostructures, UPV/EHU Science Park, 48940, Leioa, Spain

ARTICLE INFO

Keywords:
Shape memory polyurethanes
Phase change materials
Encapsulation
Thermal storage
Textile application

ABSTRACT

The present work is a first approach in order to achieve thermo-sensitive and waterproof polyurethane fibers useful in the textile industry. For this, two polyurethane formulations with glass transition temperatures (T_g) close to the body temperature have been synthetized and characterized by several techniques such as Thermogravimetric Analysis (TGA), Differential Scanning Calorimetry (DSC), Dynamic-Mechanical Analysis (DMA) and Thermo-mechanical analysis (TMA). In this manner their thermal and shape memory behavior were determined. It was also estimated the water vapor transmission rate of both polyurethane films. Then, integration of two different microencapsulated phase change materials (PCMs), one with organic shell and another one, with an inorganic shell, was carried out by extrusion in order to achieve materials with thermo-regulating properties. Fibers for both polyurethanes, pristine or loaded with microencapsulated PCMs, were again characterized to check that the thermal and shape memory properties are maintained, and to study their capability to storage and release energy. The promising results pave the way for a new generation of thermo-regulating materials useful in numerous applications such as the textile sector.

1. Introduction

People in extreme environments need clothes that can keep them warm and dry simultaneously. Thus, the study and control of thermo-regulation and humidity regulation are of extreme importance in different fields; including sportswear, underwear, and protective equipment, where user comfort needs to play a significant role [1–3]. However, traditional textiles, made from natural fibers (cotton, linen …) or synthetic fibers (polyester, nylon …) do not fulfill this function adequately. Consequently, people keep warm and dry mainly by wearing more clothing [4]. Therefore, based on the above mentioned requirements, developing smart textiles integrating thermal regulation and waterproof is highly desired.

There are two main strategies to obtain smart textiles. First, starting from an intrinsic smart material, such as a piezoelectric, electroactive or shape memory material. Second, trying to develop smart textiles using functional particles integrated into textile, which can respond to external temperature variations [5,6]. Both strategies are combined in this work in order to obtain thermo-sensitive and waterproof fibers useful in the textile industry. For this, it has been selected as intrinsic smart material a shape memory polyurethane, whereas as functional particles energy storage materials such as microencapsulated phase change materials (PCMs) were chosen.

Nowadays polyurethanes (PUs) are one of the most versatile

* Corresponding author. Departamento de Química Física, Facultad de Ciencia y Tecnología University of the Basque Country (UPV/EHU) 48940 Leioa, Spain.
E-mail addresses: josemanuel.laza@ehu.eus (J.M. Laza), antonio.veloso@ehu.eus (A. Veloso-Fernández), jsanchez903@ikasle.ehu.eus (J. Sanchez-Bodon), anem362@gmail.com (A. Martín), amaia.martinez@tekniker.es (A.M. Goitandia), cristina.monteserin@tekniker.es (C. Monteserín), xabier.mendibil@tekniker.es (X. Mendibil), karmele.vidal@tekniker.es (K. Vidal), jon.lambarri@tekniker.es (J. Lambarri), estibaliz.aranzabe@tekniker.es (E. Aranzabe), miren.blanco@tekniker.es (M. Blanco), joseluis.vilas@ehu.eus (J.L. Vilas-Vilela).

https://doi.org/10.1016/j.polymertesting.2022.107807
Received 24 June 2022; Received in revised form 12 September 2022; Accepted 26 September 2022
Available online 29 September 2022

materials, with numerous applications in different fields, such as the construction, automotive industry, biomedicine, electronics, textile sector, etc. [7]. Moreover, PUs are used in multiple appearances as adhesives, fibers, foams (rigid, semi-rigid or flexible), paints, coatings, sealants … [7,8], and these materials can be elastomers, thermoplastics or thermosets. Additionally, some polyurethanes may present the ability to store a temporary (deformed) shape and recover a 'memorized' permanent shape under an external stimulus [9,10], that is, exhibit shape-memory behavior. These shape memory polyurethanes (SMPUs) can be considered smart polymeric materials able to change their shape under a particular stimuli [9–12], such as pH, light, temperature, magnetic or electric field, solvent or irradiation, etc. The most studied of them are thermo-responsive shape-memory polyurethanes, that present the ability of modifying its shape with a temperature change. Thermo-responsive SMPUs have been intensively investigated during the past fifty years [13–22] due to their high shape recovery ratios and the easy control of their final properties by tailoring their structure, i.e. selecting the appropriate polyol, diisocyanate and chain extender that form the SS and the HS [13–15]. Nevertheless, little attention has been paid in developing SMPU fibers, mainly because it is difficult to meet the strict requirements of mechanical resistance and thermal stability demanded for fibers in the textile sector [10,23]. In addition, it is too difficult to create monofilaments due to the specific properties of PUs, such as mechanical strength, viscosity, flexibility and elasticity [24,25]. Despite of it, initial attempts to synthesize SMPU fibers from PU pellets shown that they are promising active materials for the textile industry [26].

The second strategy was to fabricate thermo-regulation smart textiles using microencapsulated phase change materials that are added into textile fibers. Phase-change materials (PCMs) are smart materials, which have the ability to store and release energy in a specific temperature range [27]. However, they have a limitation, as when they melt, the liquid phase creates problems like leakage. Microencapsulation of the PCMs solves the leakage issue by containing the liquid PCM inside an organic or inorganic shell forming a capsule with micrometer to millimeter size. This microencapsulation will also increase the surface-to-volume ratio of the PCM, improving the heat transfer of the system [28]. In this way, the use of microencapsulated PCMs (MEPCMs) with a melting point from 15 to 35 °C is a good alternative to develop durable thermo-regulating textiles [29]. Thus, when the body temperature increases, the PCM melts (as phase change takes place from solid to liquid) and absorbs the heat from the body in the form of latent heat (cooling effect). When the temperature drops, the PCM crystallizes (as phase change takes place from liquid to solid) and the stored heat is released again to the body (warming effect) [30].

The development of thermo-regulated smart textiles is of growing interest to researchers and there have been studied various techniques to incorporate PCMs into fibrous structures such as coating, lamination and electrospinning. For example, Ruiz-Calleja et al. [3] compared the thermal behavior of a cellulosic fabric when applying a coating paste containing graphene or phase change materials individually, and both together. Also in 2020, Lu et al. [4] reported some multifunctional textiles with thermo-regulation and long afterglow illumination based on phase change materials paraffin wax and phosphors: $SrAl_2O_4$: Eu^{2+}, Dy^{3+} via coaxial electrospinning approach. Nevertheless, to the best of our knowledge, there are no works where PCMs were incorporated to PU fibers in pellet form, neither where the synergy produced by using both strategies in the same shape memory polyurethane were studied.

The aim of this work is to prepare in a simple way SMPUs with transition temperatures of shape memory effect close to body temperature for its use in the textile industry. In the aforementioned previous works [13–15], the synthesis of SMPUs with a soft segment glass transition temperature close to the body temperature using the pre-polymer method was optimized. Therefore, in this work, sheets and fibers were prepared from two of the SMPUs studied before, pristine or loaded with the MEPCMs. The thermal, mechanical and shape memory properties of the SMPU fibers and sheets were determined. Loaded SMPU materials presented an interesting latent heat that increased with the MEPCM content at melting temperatures around 20 °C and 28 °C and crystallization temperatures around 7 °C and 20 °C for INOR-MEPCM and OR-MEPCM, respectively. The obtained results show that these fibers were synthetized without loss of both thermal and mechanical properties. Moreover, the shape memory behavior is also maintained with fixation (R_f) and recovery ratios (R_r) values close or higher to 90%. The water vapor permeability studies shows that these SMPUs could be attractive candidates for potential applications, such as breathable fabrics or moisture-management textiles.

2. Materials and methods

2.1. Materials and sample preparation

In this study, both polyurethanes have been synthetized by the pre-polymer method combining the three components in different molar proportions: polyol/diisocyanate/chain extender = 1/N+1/N (NCO/OH ratio 1/1 in all cases). Two polytetramethylene glycols with molecular weight of 650 g mol^{-1} (PTMG650) or 1000 g mol^{-1} (PTMG1000) were used as polyols; toluene diisocyanate (TDI) was used as an aliphatic diisocyanate; and, 1,4-butanediol (BD) was used as chain extender. All these reagents, supplied from Sigma Aldrich, were used as received except the chain extender (BD), which were dried under vacuum 24 h at 80 °C.

Two different microencapsulated phase change materials (MEPCMs) were employed. The main phase change properties of selected phase change microcapsules are collected in Table 1. All data were determined by differential scanning calorimetry and thermogravimetric analysis at a heating rate of 10 °C·min^{-1} in nitrogen atmosphere. The first material is an acrylate-based organic shell microencapsulated phase change material (OR-MEPCM) in form of dry powder, with the commercial name Micronal® DS 5038 X, obtained from BASF. It has a first small melting transition at around −1.5 °C and a second main transition at temperatures in the comfort range, at around 28 °C. The second MEPCM is an inorganic microencapsulated phase change material (INOR-MEPCM) with a hexadecane core and a silica shell structure, also in the form of a dry powder. The procedure for the preparation of these encapsulated PCM has been previously reported [29]. The SEM images of both MEPCMs are collected in Fig. S1. Inorganic MEPCM possess a homogeneous size distribution with diameters around 500 nm, whereas organic ones have a more heterogeneous distribution with diameters between 3 and 6 μm.

For the synthesis of both polyurethanes, first the polyol (PTMG650 or PTMG1000) reacts with the diisocyanate (TDI) to obtain an intermediate polymer, called pre-polymer. Then, the chain extender (BD) is added to the reaction medium allowing the polyurethane chains to grow. In Table S1 (Supplementary Information) are summarized both SMPU compositions. These synthesis takes place as previously reported [13,14]. Briefly, during 2 h at 80 °C, the polyol and the isocyanate were stirred in a 250 mL five-neck round bottom flask equipped with a nitrogen inlet and a mechanical stirrer, obtaining the pre-polymer. Next, the chain extender (BD) was added allowing it to react for 8–10 min. Finally, the obtained low molecular weight polyurethane was poured into a stainless steel mold (dimensions: 50 mm × 50 mm x 1.5 mm). Two Teflon sheets were placed on both sides of the metallic mold to reduce the surface roughness of the obtained PU sheets. This mold was placed into a hydraulic press (100 °C, 100 bar) for about 20 h. After that time, the final PUs were obtained cooling at room temperature. These polyurethane sheets were used to prepare the additivated fibers, but also to prepare 0.25 mm thick polyurethane films for the water vapor transmission rate (WVTR) measurements.

To prepare the fibers (Table 2), first, it is necessary to cut the polyurethane sheets obtained in the press into small pieces (no more than 0.5 cm^2). These polyurethane pellets were transformed into fibers by

Table 1
Main thermal properties of selected microencapsulated phase change materials.

	T_m (°C)			ΔH_m (J/g)	T_c (°C)			ΔH_c (J/g)	T_d (°C)
	T_{onset}	T_{peak}	T_{endset}		T_{onset}	T_{peak}	T_{endset}		
INOR-MEPCM	15.2	21.7	28.9	127.1	15.4	11.1	2.50	125.0	180
OR-MEPCM	−4.0	−1.5	2.5	14.4	−3.5	−5.8	−9.6	13.5	163
	22.73	28.0	35.8	117.6	25.6	19.8	10.9	122.3	192

T_m: melting temperature obtained by DSC, T_c: crystallization temperature obtained by DSC, T_{onset} = temperature at which the process starts, T_{peak} = temperature at which the peak of the process occurs, T_{endset} = temperature at which the process ends, ΔH_m: melting enthalpy, ΔH_C: crystallization enthalpy, T_d = degradation temperature obtained by TGA.

Table 2
Polyurethane fibers compositions.

Fiber Code	PCM (wt.%)	
	OR-MEPCM	INOR-MEPCM
PTMG650-TDI-BD N3	–	–
PTMG650-TDI-BD N3 10% OR-MEPCM	10	–
PTMG650-TDI-BD N3 10% INOR-MEPCM	–	10
PTMG650-TDI-BD N3 30% OR-MEPCM	30	
PTMG650-TDI-BD N3 30% INOR-MEPCM		30
PTMG1000-TDI-BD N5	–	–
PTMG1000-TDI-BD N5 10% OR-MEPCM	10	–
PTMG1000-TDI-BD N5 10% INOR-MEPCM	–	10
PTMG1000-TDI-BD N5 30% OR-MEPCM	30	–
PTMG1000-TDI-BD N5 30% INOR-MEPCM	–	30

using a correlating conical twin screw micro-extruder (Haake Minilab II) with an integrated backflow channel to adjust the material residence time and with a die diameter of 0.5 mm. Fibers from pristine polyurethanes, PTMG650-TDI-BD N3 and PTMG1000-TDI-BD N5, and polyurethanes modified with 10 and 30 wt% of both microencapsulated PCMs were obtained at 175 °C with a screw rotation speed of 15 rpm. The samples were maintained re-circulating for 5 min inside the extruder to allow a good dispersion of microcapsules in the polymeric matrices.

2.2. Characterization

All PUs (Table S1) were characterized by different techniques in order to know the thermal and mechanical properties, as well as, evaluate the shape memory capacity. The obtained fibers (pristine or modified with both type of MEPCMs) were characterized in the same way.

2.2.1. Thermal analysis (TGA, DSC)

Mettler Toledo TGA/SDTA851e thermobalance was employed to evaluate the thermal stability in a similar way as previously described [14,15]. Several parameters such as the initial degradation temperature (T_i), the temperature for each degradation step (T_{d1}, T_{d2}, …) and the final residue are evaluated. TGA experiments were done in duplicate.

A Mettler Toledo model DSC 822e calorimeter was used to determined the thermal properties of each PU sample [13]. Samples around 10 mg were subjected to a heating/cooling/heating cycle from −100 to 250 °C for the pristine polyurethanes or to a heating/cooling cycle from −50 to 50 °C for those polyurethanes loaded with MEPCMs, at a scanning rate of 10 °C·min^{-1} under constant nitrogen flow (20 mL min^{-1}). These tests were also done in duplicate.

2.2.2. Thermal analysis (DMA, TMA, tensile test)

DMA tests were perfomed twice in tensile mode (DMA-1 Mettler Toledo equipment). PU specimens with dimensions 1.5 mm thick, 5 mm wide and 10 mm long (for the fibers the dimensions are 0.5 × 0.5 × 10 mm) were prepared. These specimens were measured at a heating rate of 3 °C·min^{-1} from −100 °C to 100 °C using a 10 Hz deformation frequency and a displacement (20 μm) that are within the linear viscoelastic region (LVR) of the synthetized PUs [13,15].

For thermo-mechanical analysis (TMA), DMA-1 Mettler Toledo equipment in tensile mode was also employed. To evaluate the shape memory capacity of the synthetized PUs, as it has been reported previously [13,14], the temperature range chosen to perform the TMA tests must be below and above the temperature that active the shape memory effect, which in this work is the glass transition temperature measured by DMA, Tg-peak. Briefly, a rectangular sample was heated above $T_{g\text{-}peak}$ of the sample tested, and then was elongated by the action of a 2 N force. Then, the maximum elongation can be measured (ε_m). After, keeping the force constant, the sample was cooled quickly below its $T_{g\text{-}peak}$, in order to fix the temporary shape (ε_u) once this force was removed. In the recovery step, the sample was reheated above its $T_{g\text{-}peak}$ to recover its permanent shape (ε_p). Therefore, the deformation (R_d), fixation (R_f) and recovery (R_r) ratios were calculated from the same equations reported previously [15].

The tensile testing was carried out using a MTE-1 Testing Machine from Techlab Systems in tensile mode. PU fibers with 5 mm long, 0.5 mm thick and 0.5 mm wide were tested. The capacity of the used load cell was 500 N, while the test speed was 10 mm min^{-1}. Young's modulus (E), stress and strain at yield (σ_y, ε_y) and stress and strain at break (σ_b, ε_b) were determined at room temperature (about 20 °C). Reported values represent mean average values and standard deviations over 5 specimens.

2.2.3. Water vapor transmission rate (WVTR) measurement

The capability of the PU films to be used as water barrier was tested by measurements of water vapor transmission rate (WVTR) [31]. WVTR tests were conducted using a modified ASTM procedure [32]. In this way, the PU films were placed sealing glass vessels (3.5 cm diameter) containing 25 g of immediately previously dried silica gel. These glass vessels were stored in a climatic chamber at high relative humidity (about 90%) above and below T_{trans}. WVTR was finally determined by weight gain in silica gel according to equation (1) [33,34].

$$WVTR = \frac{w \cdot x}{A \cdot t \cdot (p_2 - p_1)} \left[\frac{g \cdot mm}{m^2 \cdot day}\right] \quad (1)$$

where x is film thickness (0.25 mm), w is the weight gain, A is the area of exposed PU film (approx. 9.6 cm^2), t is the measurement time and p_2-p_1 is the vapor pressure differential across the PU film. Measurements were made thrice, and the average WVTR was reported.

2.2.4. Scanning electron microscope (SEM)

The morphologies of the microencapsulated PCMs and polymeric fibers with the microencapsulated PCMs were studied by scanning electron microscopy (SEM) using an Ultra Gemini-II microscope from Carl Zeiss SMT. The samples are maintained in a fridge at 6 °C and them cut with the help of a razor for the analysis.

2.2.5. Dynamic heat transfer with a thermal camera

Dynamic thermal analysis was performed to confirm the surface temperature changes (the cooling delay effect and time lag) in specimens of SMPU modified with MEPCMs. It was performed using a data

logger and a thermographic camera optris xi400 model, with microbolometer. A heated surface was used as a heat source to measure dynamic heat transfer. Specimens of PTMG1000-TDI-BD N5 polymer modified with 10–30 wt% of INOR-MEPCM and 30 wt% of OR-MEPCM, have been obtained by injection in a Haake minijet at 180 °C using 800 bar of pressure. The mold temperature was maintained at 60 °C. The specimens were circular with a diameter of 35 mm and a thickness of 1.5 mm. The specimens were heated at 60 °C in an oven for 10 min and then, they are slowly cooled in a cold room with a temperature set at 6 °C. The cooling process was recorded continuously.

3. Results and discussion

3.1. Polyurethane sheets

First, based on our previous experience [13–15], two polyurethane formulations indicated in Table S1 were synthetized. Both PU formulations were synthetized both in sheet (1.5 mm thick) and in films (0.25 mm thick) shape. So, the PU sheets were characterized by several techniques as thermogravimetric analysis, differential scanning calorimetry, dynamic-mechanical analysis, and thermo-mechanical analysis. Besides, the water vapor transmission rate (WVTR) of the PU films were evaluated using a climatic chamber.

As can be seen in Table S2 (Supplementary Information), both PUs have a high enough thermal stability to be processed in fibers without undergo degradation processes. The initial degradation temperatures (T_i), taken as the temperature at which the mass loss is 1 wt%, are 273.1 and 262.7 °C for PTMG650-TDI-BD N3 and PTMG1000-TDI-BD N5 samples, respectively, much higher than the transformation temperature of PU into fiber (approx. 175 °C). From TGA curves (Fig. S2 in Supplementary Information), the degradation temperatures of each of the two main degradation steps of the polyurethane can also be determined. The first, due to the hard segment, is between 360 and 390 °C, while the soft segment one is between 440 and 470 °C.

From DSC analysis (Table S2 and Figure S3 in Supplementary Information), a first estimation of the glass transition temperature can be made in order to check its adequation for a possible future application in the textile industry. In both cases, $T_{g\text{-endset}}$ values slightly below or above the body temperature were observed, 33.6 and 43.6 °C for PTMG650-TDI-BD N3 and PTMG1000-TDI-BD N5 samples, respectively. These T_g values were confirmed by DMA (Table S2 and Figure S4 in Supplementary Information), with $T_{g\text{-peak}}$ values 33.0 and 45.3 °C, respectively.

Finally, Table S2 summarizes the calculated values that quantifies the shape memory behavior of both PU samples, the deformation (R_d), fixation (R_f) and recovery (R_r) ratios. The TMA curves are presented on Fig. S5 in Supplementary Information. As can be seen on Table S2, the deformation ratio (R_d) produced by applying a force of 2 N is around 14–15% for both PUs. The ability to fix a temporary shape is estimated from R_f values. Both PUs have fixation ratios higher than 92%, which, taking into account the applied deformations (around 15%) can be considered acceptable values. Furthermore, the synthetized PUs show a high ability to recover their original shape, above 95% (Table S2). In conclusion, both synthetized polyurethanes have good shape memory effect with transition temperatures of shape memory effect close to body temperature.

Additionally, the water vapor transmission rate (WVRT) was measured in polyurethane films (0.25 mm thick). These measurements were made below and above the transition temperature of the shape memory effect of polyurethanes, that is, below and above their glass transition temperature measured by DMA ($T_{g\text{-peak}}$ in Table S2). Briefly, the glass vessels (3.5 cm diameter), sealed with the PU films and containing 25 g of immediately previously dried silica gel, were prepared in triplicate and weighed. After, they were put in a climatic chamber at high relative humidity (about 90%) at 20 °C during 24 h. Then they were weighed, and were put again back in the climatic chamber at 30 °C during other 24 h. This process was repeated at 40, 50, 60, 70 and 80 °C (the latter temperature much higher than the T_g of the material).

Finally, applying equation (1) the water vapor transmission rate (WVRT) of both polyurethanes in function of temperature can be estimated (Fig. S6 in Supplementary Information). It can be seen in Fig. S6 that WVTR increases with temperature for both polyurethane samples. As it is well known, the diffusivity of water vapor is influenced by the internal porosity of the samples (free volume) [35–38]. Moreover, in previous studies [39,40], the authors have studied the connection among free volume and the shape memory effect in shape memory polyolefins, observing that it rise with the temperature favoring the movement of the molecules and allowing its reorganization during the macroscopic shape recovery up the transition temperature of the shape memory effect.

At temperatures below the transition temperature of the shape memory effect (20–30 °C), the diffusivity of the water vapor in both polyurethanes is near zero. When temperature rises, the free volume rises and therefore the diffusivity, showing the materials a higher transmission of water vapor. So, the WVTR values for temperatures above the transition temperature of the shape memory effect are about 10–15 times higher than before. This increase in WVTR, as mentioned before, is derived from the rise of intermolecular chain space due to the increase of the molecular chain mobility.

However, for PTMG650-TDI-BD N3 sample it is observed a decrease in WVTR at 80 °C. This behavior could be explained looking Fig. S4 in Supplementary Information. Tanδ in DMA curve show an increase up to 70 °C indicating a change in the internal structure of the material, which becomes softer and more viscous. This causes the pores to close making the transmission of water vapor difficult and, therefore, lowering the WVTR value.

In conclusion, the porosity to water vapor increases several orders of magnitude when the samples are heated above the transition temperature of the shape memory effect of PU samples (up to body temperature). This is a noteworthy fact that opens up these polyurethane materials to very interesting and fascinating opportunities in the textile industry.

3.2. Polyurethane fibers

As it is explained in the materials and sample preparation part, sheets of the two polyurethane formulations selected to make the fibers (PTMG650-TDI-BD N3 and PTMG1000-TDI-BD N5), have been cut into small pieces (no more than 0.5 cm^2). These pellets have been mixed in a microextruder with 10–30 wt% of both MEPCMs. Initially, the thermal performance of the modified MEPCM polymeric systems has been tested using a thermal camera by dynamic thermal analysis. Specimens of PTMG650-TDI-BD N3 polymer modified with 10–30 wt% of INOR-MEPCM and 30 wt% of OR-MEPCM, obtained by injection moulding, were heated at 60 °C for 10 min. Then, it was recorded the cooling process of the specimens in a camera at 6 °C. Fig. 1 shows the thermographic images showing the change in surface temperature during free cooling of the specimens, and Fig. 2 shows the graphical representation of the temperature evolution during the free cooling process.

The results indicated that the presence of MEPCM delayed the free cooling process of the reference material. For the polymer modified with the INOR-MEPCM the delay starts at temperatures between 12 and 15 °C, whereas for the polymer modified with the OR-MEPCM the delay occurs at temperatures around 25 °C. Moreover, in case of the polymer modified with 10–15 wt % of INOR-MEPCM, it can be observed that when the amount of MEPCM in the material increased, it occurs a decrease in the temperature loss due to the fact the MEPCM preserve the heat during the free cooling process due to its latent heat storage capability.

Once thermoregulating properties of these materials have been tested, the obtained pellets were employed to manufacture fibers loaded or not with the microencapsulated phase-change materials (MEPCMs) (Table 2). These PU fibers were characterized by the same techniques previously described for the PU sheets: thermogravimetric analysis

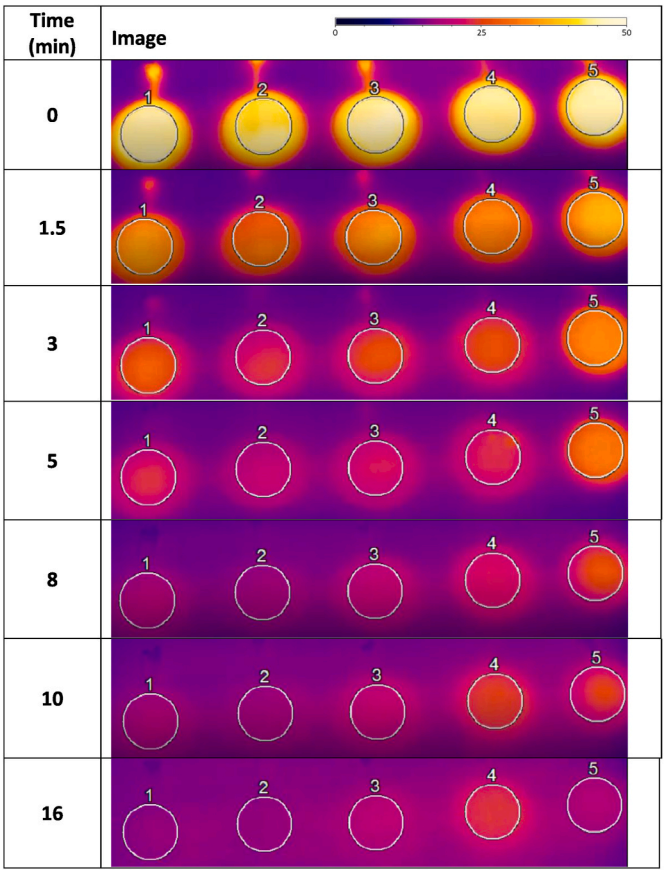

Fig. 1. Surface temperature behavior depicting heat storage of MEPCM modified PTMG1000-TDI-BD N5 polymer: 1. reference; 2. 10 wt% INOR-MEPCM; 3. 20 wt% INOR-MEPCM; 4. 30 wt% INOR-MEPCM and 5. 30 wt% OR-MEPCM.

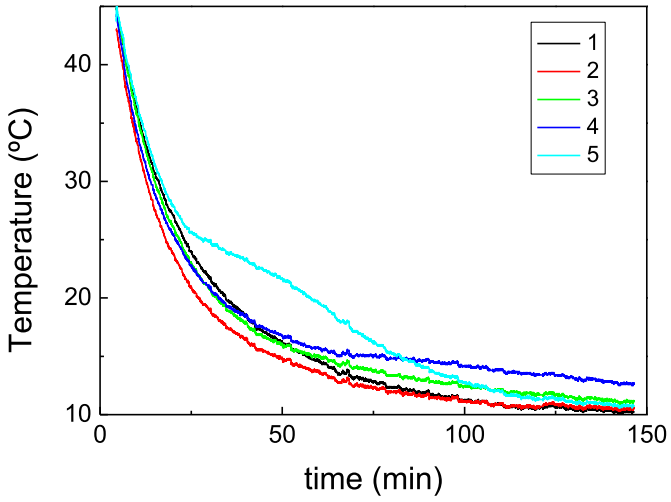

Fig. 2. Temperature evolution on the surface of the specimens of MEPCM modified PTMG1000-TDI-BD N5 polymer: 1. reference; 2. 10 wt% INOR-MEPCM; 3. 20 wt% INOR-MEPCM; 4. 30 wt% INOR-MEPCM and 5. 30 wt% OR-MEPCM.

(TGA), differential scanning calorimetry (DSC), dynamic-mechanical analysis (DMA), and thermo-mechanical analysis (TMA). Moreover, tensile properties were measured, and SEM images were taken in order to check the well distribution of the PCMs into the fibers.

In Fig. 3, the SEM images of the PTMG650-TDI-BD N3 fibers, unmodified and modified with 30 wt% of the organic and inorganic MEPCMs are observed (SEM images of the microencapsulated phase-change materials in Fig. S1 in Supplementary Information). For the unloaded fibers, the SEM images showed a continuous surface, being observed the marks of the razor employed to cut the specimens, while for the fibers modified with 30 wt% of both type of MEPCMs, there can be observed the microcapsules homogenously distributed in the fibers. The fibers of PTMG650-TDI-BD N3 modified with 30 wt% of OR-MEPCM shows the presence of capsules between 3 and 6 μm, as it was expected, and some holes which could have been generated by some microcapsules that left the samples during the specimen preparation.

Similarly, for PTMG650-TDI-BD N3 fibers modified with 30 wt% of INOR-MEPCM homogeneously distributed microcapsules with a diameter lower than 1 μm are observed and some larger holes of around 2–3 μm corresponding to aggregated nanoparticles. Due to the synthesis method, a small amount of the inorganic nanoparticles could be joined by the inorganic shell, forming a larger aggregate of nanoparticles. Similar images are obtained for the fibers using PTMG1000-TDI-BD N5 polyurethane (Fig. S7 in Supplementary Information).

Table 3 shows the main thermal characteristics of the PU fibers measured both by TGA and DSC. It can be seen that the initial degradation temperatures (T_i), taken as the temperature at which the mass loss is 1 wt%, decreases considerably in loaded fibers compared to unloaded fibers. However, although the temperature for each degradation step (T_{d1} for the hard segment, and T_{d2} for the soft segment) also decrease, this decrease is less than in T_i, being only slightly smaller in the degradation step of the soft segment (T_{d2}). Moreover, as can be seen in Fig. 4, the first degradation step really begins for all fibers among 250–300 °C, which indicate that the lower values in T_i may be due to the possible presence of water or to a small leakage/evaporation of PCMs from the material during heating. Anyway, the PU fibers loaded or not with PCMs have high enough thermal stability for its future application as smart materials in the textile sector.

$T_{g\text{-onset}}$ and $T_{g\text{-endset}}$: respectively glass transition temperatures at which the process starts and at which the process ends measured by DSC (Fig. S8). $T_{m\text{-peak}}$: melting temperature obtained by DSC in the heating scan, T_c: crystallization temperature obtained by DSC in the cooling scan, ΔH_m: melting enthalpy measured by DSC in the heating scan, ΔH_C: crystallization enthalpy measured by DSC in the cooling scan (Fig. 5).

The glass transition temperature of all the PU fibers, obtained from DSC analysis, are shown in Table 3 (and Fig. S8 in Supplementary Information). As it can be seen, these $T_{g\text{-endset}}$ values are not greatly modified when the polyurethanes are processed from pellets to fibers: 33.6–35.3 °C for PTMG650-TDI-BD N3 sample and 43.6 to 41.1 °C for PTMG1000-TDI-BD N5 sample, respectively. However, when the fibers are loaded with the inorganic PCMs a slight decrease in T_g values were observed, that is higher as the percentage of added PCMs increases. For example, for the PTMG650-TDI-BD N3 sample, $T_{g\text{-endset}}$ diminish from 35.3 °C to 29.0 °C and to 20.5 °C when 10 and 30 wt% of PCMs is added, respectively. This may be due to the water plasticizing effect or PCM leached during heating (observed in the TGA measurements). The same behavior is seen for the PTMG1000-TDI-BD N3 sample. For organic PCMs it is not possible to observe this effect because they present an endothermic melting peak (Fig. 5 and Fig. S8), more intense when the percentage of PCMs is higher, just at the temperatures where the glass transition temperature should appear.

Table 3 also shows the ability to store and release energy of those polyurethanes loaded with MEPCMs. For this, both the melting and crystallization temperatures (T_m, T_c) and their corresponding enthalpies (ΔH_m, ΔH_c) are determined by DSC (Fig. 5). Thus, it is observed that both T_m and T_c of the samples loaded with OR-MEPCM (29 and 21 °C, respectively) are higher than those obtained with INOR-MEPCM (20 and 7 °C, respectively). On the other hand, the melting and the cooling enthalpies are higher for the SMPUs loaded with OR-MEPCM (between 5-7 and 25–34 J g^{-1} for those samples loaded with 10 and 30 wt%, respectively). Therefore, a new generation of synthetized SMPU fibers that can act as future active materials with applications in the textile

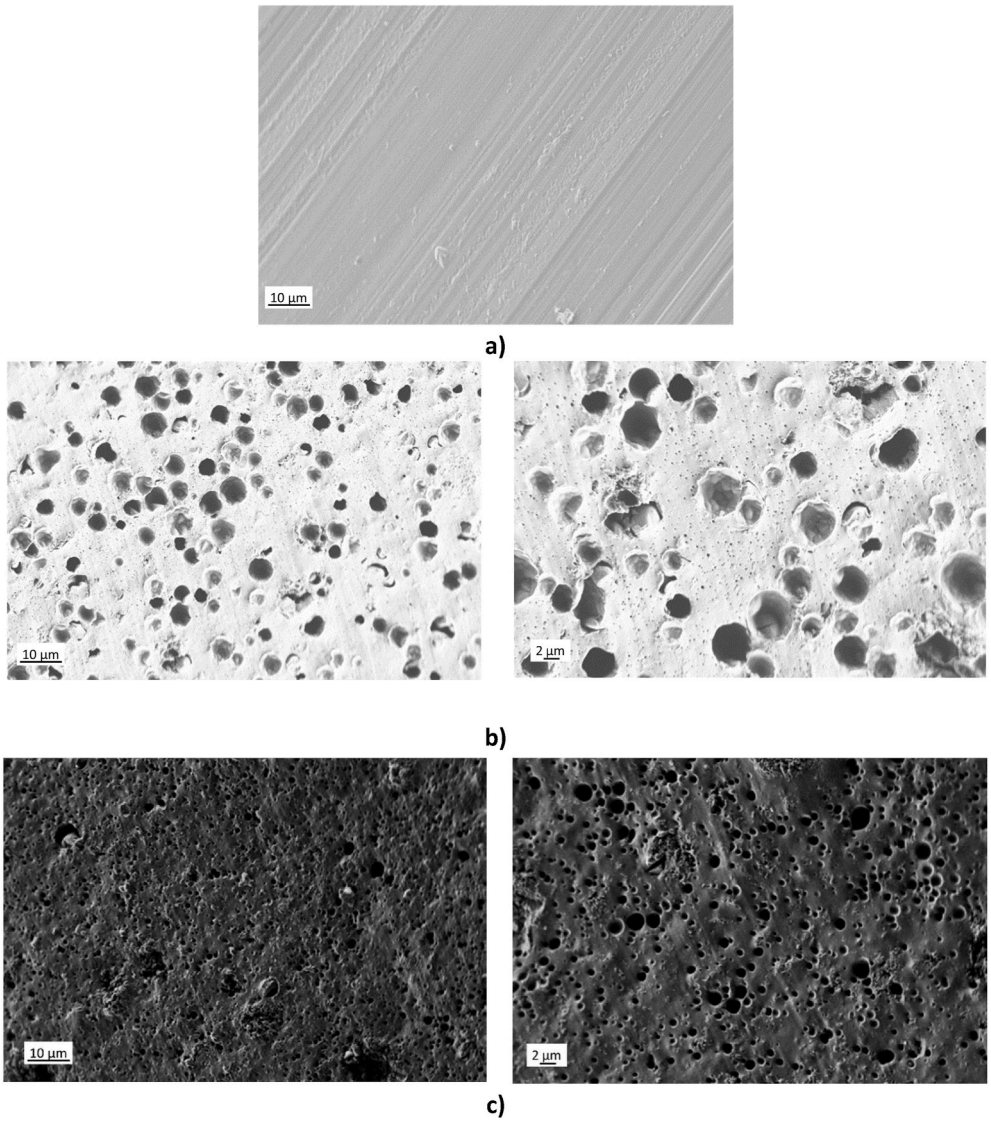

Fig. 3. SEM images of fibers of PTMG650-TDI-BD N3: a) pristine, b) modified with 30 wt% of OR-MEPCM, and c) modified with 30 wt% of INOR-MEPCM.

Table 3
Main thermal characteristics of PU fibers.

Fiber Code	TGA			DSC					
	T_i (°C)	T_{d1} (°C)	T_{d2} (°C)	$T_{g\text{-onset}}$ (°C)	$T_{g\text{-endset}}$ (°C)	$T_{m\text{-peak}}$ (°C)	ΔH_m (J/g)	$T_{c\text{-peak}}$ (°C)	ΔH_c (J/g)
PTMG650-TDI-BD N3	273.3	387.1	465.3	19.2	35.3	–	–	–	–
PTMG650-TDI-BD N3 10% OR-MEPCM	140.5	288.9	420.0	–	–	28.8	7.4	20.9	−7.4
PTMG650-TDI-BD N3 10% INOR-MEPCM	83.0	289.4	421.1	5.1	29.0	19.1	2.5	7.48	−2.5
PTMG650-TDI-BD N3 30% OR-MEPCM	169.5	246.2	370.1	–	–	28.5	33.0	19.6	−34.0
PTMG650-TDI-BD N3 30% INOR-MEPCM	170.6	255.7	371.0	5.5	20.5	21.2	20.9	6.03	−20.4
PTMG1000-TDI-BD N5	262.7	368.3	450.6	25.2	41.1	–	–	–	–
PTMG1000-TDI-BD N5 10% OR-MEPCM	152.2	286.7	417.1	–	–	28.8	4.38	21.7	−4.8
PTMG1000-TDI-BD N5 10% INOR-MEPCM	134.5	291.0	413.8	13.6	38.1	20.5	0.6	–	–
PTMG1000-TDI-BD N5 30% OR-MEPCM	158.2	242.3	364.2	–	–	27.9	24.9	21.3	−26.2
PTMG1000-TDI-BD N5 30% INOR-MEPCM	118.1	249.1	363.1	17.3	23.1	19.6	15.8	7.0	−13.1

T_i: initial degradation temperature obtained by TGA, T_{d1} and T_{d2}: initial degradation temperatures for each degradation step obtained by TGA (Fig. 4).

industry could be obtained with both MEPCMs, selecting the more appropriate additive for the final application as a function of the most suitable melting/crystallization temperature of the SMPU fibers. If fibres are used in colder climates, the performance of the fibres with INOR-MEPCM that present a lower temperature would be more suitable. The amount of MEPCM will be determined as a balance between the mechanical properties of the fibers and the thermal performance required for the specific application of the textile.

The T_g values were also measured by DMA (Table 4 and Fig. 6), with $T_{g\text{-peak}}$ values 52.7 and 57.2 °C for PTMG650-TDI-BD N3 and PTMG1000-TDI-BD N5 samples, respectively. On the other hand, when the fibers are loaded with the PCMs a slightly variation in $T_{g\text{-peak}}$ values

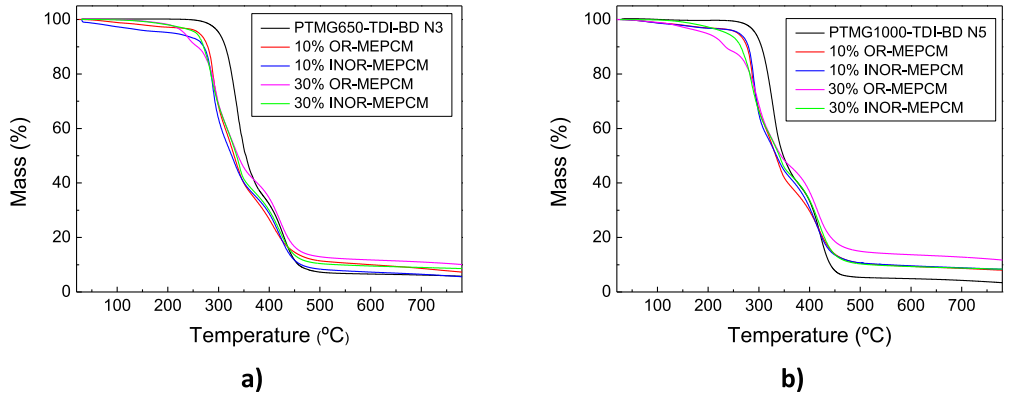

Fig. 4. TGA curves for all PU fibers, loaded with PCMs or not. a) PTMG650-TDI-BD N3 fibers, and b) PTMG1000-TDI-BD N5 fibers.

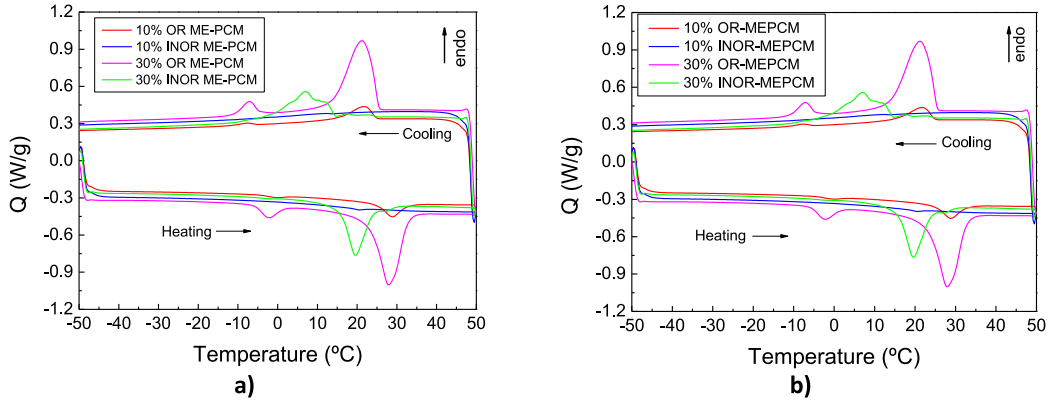

Fig. 5. DSC curves for all PU fibers loaded with PCMs. a) PTMG650-TDI-BD N3 fibers, and b) PTMG1000-TDI-BD N5 fibers.

Table 4
DMA results and shape memory behavior of PU fibers.

Fiber Code	DMA	TMA		
	$T_{g\text{-}peak}$ (°C)	R_d (%)	R_f (%)	R_r (%)
PTMG650-TDI-BD N3	52.7	15.7	90.4	99.5
PTMG650-TDI-BD N3 10% OR-MEPCM	50.5	15.6	89.5	99.5
PTMG650-TDI-BD N3 10% INOR-MEPCM	51.0	15.7	85.5	99.5
PTMG650-TDI-BD N3 30% OR-MEPCM	57.8	15.6	81.1	99.0
PTMG650-TDI-BD N3 30% INOR-MEPCM	53.3	15.6	89.2	99.2
PTMG1000-TDI-BD N5	57.2	15.3	89.5	99.2
PTMG1000-TDI-BD N5 10% OR-MEPCM	53.7	15.4	89.0	99.3
PTMG1000-TDI-BD N5 10% INOR-MEPCM	46.0	15.4	88.2	99.2
PTMG1000-TDI-BD N5 30% OR-MEPCM	60.5	15.6	83.6	99.0
PTMG1000-TDI-BD N5 30% INOR-MEPCM	52.5	15.6	81.4	99.2

were observed. However, by DMA the decrease in $T_{g\text{-}peak}$ seen in DSC is not observed. These different T_g values between DSC and DMA could be explained, as it has been reported previously [13,41], from the experimental point of view due to the differences between DSC and DMA. In fact, it has been demonstrated in macromolecular materials that methods such as DSC are less sensitive to the glass transition phenomenon than the DMA. Therefore, in the same way it was done for the PU sheets, the values measured by DMA ($T_{g\text{-}peak}$ in Table 4) have been into account in order to compare the values of glass transition temperature for the PU fibers. These values have been considered to perform the TMA tests that are explained below.

Finally, in Table 4 the deformation (R_d), fixation (R_f) and recovery (R_r) ratios calculated all PU fibers are summarized. TMA curves can be seen on Fig. 7. For all PU fibers the deformation ratio (R_d) is around 15.5–15.6%, quite similar to that produced in the PU sheets. R_f values, which measures the ability to fix the temporary shape, are close to 90% for all fibers; whereas R_r, estimates the ability to recover the original shape, is above 99%. In conclusion, these values are not very different from those previously observed in polyurethane sheets, so it can be assert that the PU fibers retain the shape memory effect of the starting materials.

These PU fibers are designed as a potential smart materials for their future application in the textile industry. Therefore, it is important to know their mechanical properties. For it, tensile test have been carried out as described above. Table 5 show the Young's modulus (E), stress and strain at yield (σ_y, ε_y) and stress and strain at break (σ_b, ε_b) values determined at room temperature, while Fig. 8 show the tensile curves.

In general, all fibers show an elastomeric behavior at low deformations, which becomes plastic behavior when the strain increases. Just as the elastic region is small for all fibers, the plastic region is much larger. It was also observed that elongation at break is higher than 300% in almost all PU fibers. So, PTMG650-TDI-BD N3 fiber show the highest deformation at break (1557%). On the other hand, in general,

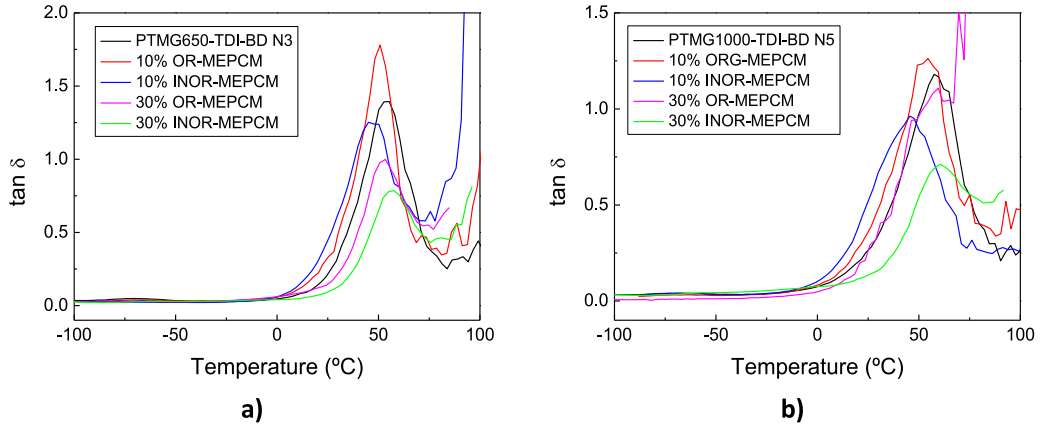

Fig. 6. DMA curves for all PU fibers, loaded with PCMs or not. a) PTMG650-TDI-BD N3 fibers, and b) PTMG1000-TDI-BD N5 fibers.

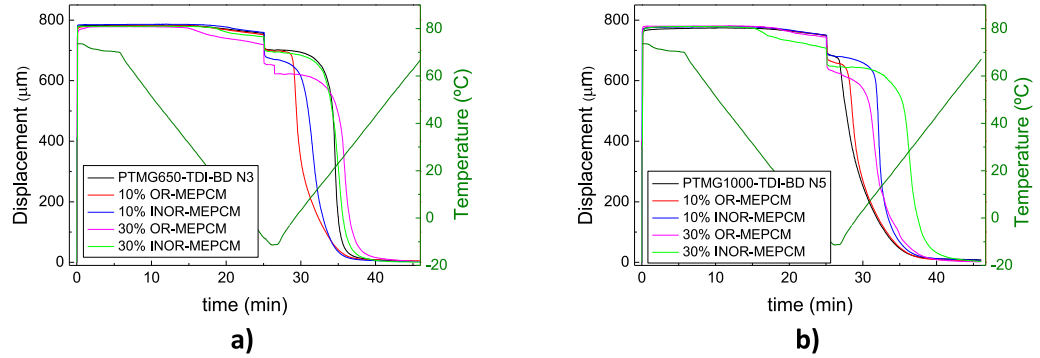

Fig. 7. TMA curves for all PU fibers, loaded with PCMs or not. a) PTMG650-TDI-BD N3 fibers, and b) PTMG1000-TDI-BD N5 fibers.

Table 5
Tensile properties for all PU fibers, loaded with PCMs or not.

Sample Code	Tensile Properties				
	E (MPa)	σ_y (MPa)	% ε_y	σ_b (MPa)	% ε_b
PTMG650-TDI-BD N3	1.25 ± 0.02	1.88	17.71	18.43	1557.7
PTMG650-TDI-BD N3 10% OR-MEPCM	0.93 ± 0.04	0.29	4.27	4.87	615.9
PTMG650-TDI-BD N3 10% INOR-MEPCM	1.36 ± 0.02	1.23	10.32	11.30	959.3
PTMG650-TDI-BD N3 30% OR-MEPCM	0.18 ± 0.05	0.44	2.74	6.53	505.7
PTMG650-TDI-BD N3 30% INOR-MEPCM	0.29 ± 0.09	1.43	7.37	5.98	283.3
PTMG1000-TDI-BD N5	0.73 ± 0.01	0.67	10.42	8.31	507.5
PTMG1000-TDI-BD N5 10% OR-MEPCM	0.89 ± 0.02	0.85	10.01	8.62	635.7
PTMG1000-TDI-BD N5 10% INOR-MEPCM	0.83 ± 0.02	0.65	9.06	3.39	284.0
PTMG1000-TDI-BD N5 30% OR-MEPCM	0.20 ± 0.05	0.89	5.77	6.45	598.7
PTMG1000-TDI-BD N5 30% INOR-MEPCM	0.23 ± 0.04	0.86	4.73	6.01	457.4

PTMG650-TDI-BD N3 fibers have higher elastic modulus than PTMG1000-TDI-BD N5 fibers. This may be due to how PUs are synthetized; the reagents used during its process of synthesis influence in the ratio between the soft and the hard segments. Thus, while the soft segment tends to orient in the direction of stretch, the hard segment remains perpendicular to the stretch direction [42,43].

If Young's modulus is observed, it drops drastically when the fibers are loaded with 30% PCMs. In the same way, strain at yield (ε_y) decreases. This may be due, in addition to the presence of PCM particles in the polymeric matrix, to the water introduced into the fibers during their processing (fact already observed by DSC and TGA).

Taking into account that the main factors that influence the final end uses of the PU fibers are the durability, elongation, tactile properties and processability [44], it could be said that the tensile properties of PU fibers synthetized in the laboratory are good enough for applications in the textile industry, such as thermo-responsive fibers. As example, several knitted smart fabrics, with different grammages, have already been obtained from these samples loaded with these microencapsulated phase change materials (Fig. 9).

Further, thermal imaging camera revealed that an increase in the proportion of MEPCMs leads to a slower decrease in temperature because of the heat preserved by MEPCMs over time.

4. Conclusions

As general conclusion, in this work it can be assessed that two polyurethane formulations, with transition temperatures of shape memory effect close to body temperature, have been successfully processed in fiber form in a simple way without loss of both thermal and mechanical properties. Moreover, the shape memory behavior of this kind of polyurethanes is also maintained with fixation (R_f) and recovery ratios (R_r) values close or higher to 90%. On the other hand, the permeability of these materials to water vapor has been estimated, showing an interesting change in this parameter down and up the glass

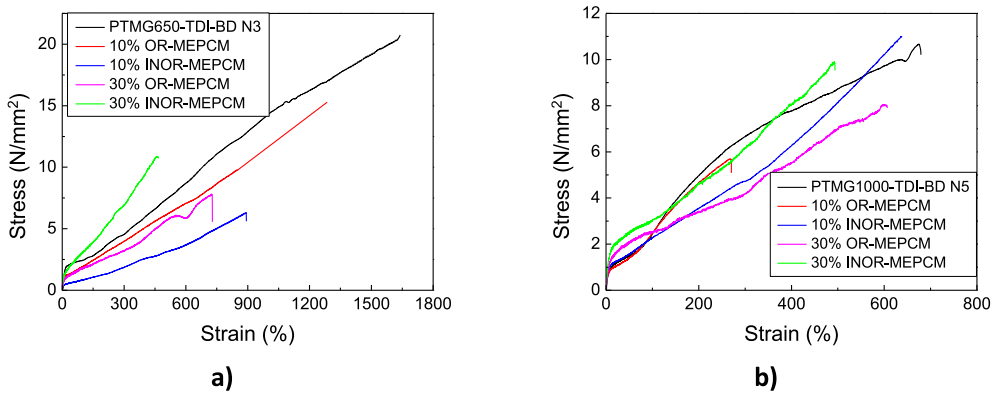

Fig. 8. Tensile tests for all PU fibers, loaded with PCMs or not. a) PTMG650-TDI-BD N3 fibers, and b) PTMG1000-TDI-BD N5 fibers.

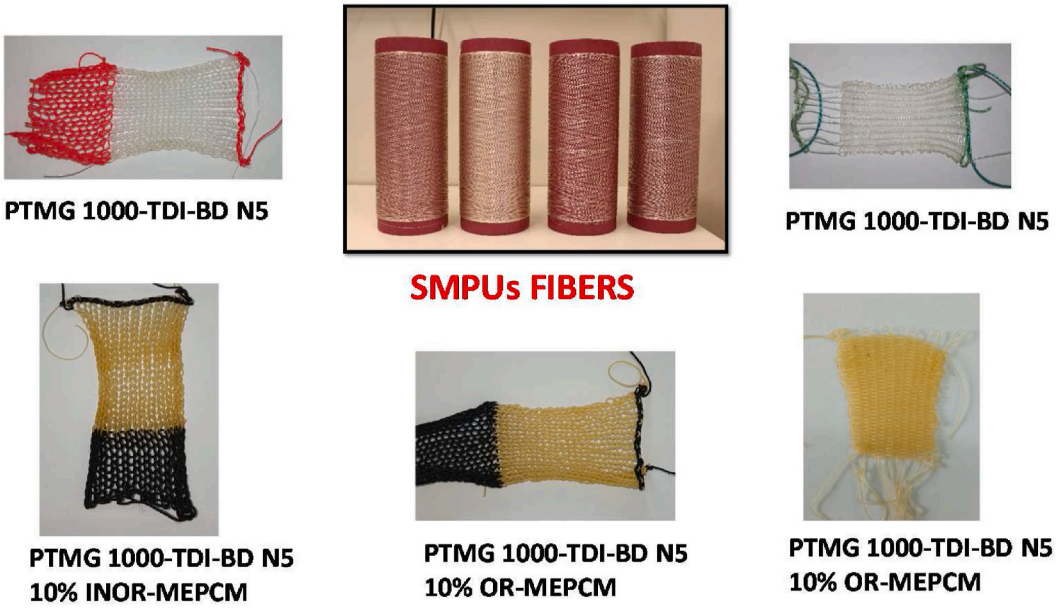

Fig. 9. Knitted smart fabrics obtained from several samples loaded with the microencapsulated phase change materials.

transition temperature, T_g (that in these materials match with the temperature that active the shape memory effect). Finally, these PU fibers have been loaded with two different microencapsulated phase-change materials, checking that the synergistic influence of both effects, shape memory and phase-change, not affect the main properties of the SMPU fibers developed. Moreover, the proper selection of the MEPCMs can allow the operation of these materials in a different temperature range, from 15 to 35 °C, being a good alternative to develop durable thermo-regulating textiles for different operational conditions. As an example, for urban textiles, taking body temperature as a reference, the sample PTMG650-TDI-BD N3 loaded with 30 wt% OR-MEPCM could be a good alternative due to the glass transition temperature of the pristine polyurethane (20–35 °C), its melting and crystallization temperatures (28 and 20 °C, respectively), and its higher melting and cooling enthalpies (around 33–34 J g^{-1}). The research carried out in this paper showed that these materials are an attractive way to make thermo-regulating and waterproof textiles, opening new lines of research on thermoregulation in textiles by combining these two materials in the same fiber.

Funding

This research did not receive any specific grant from funding agencies in the public, commercial, or not-for-profit sectors.

Author contributions

J.M.L.: DMA and TMA analysis, conceptualization and writing. A. V–F.: Conceptualization, writing and review. J.S–B.: Tensile analysis. A. M.: SMPU synthesis, WVTR measurements, and TGA, DSC analysis. A.M. G.: MEPCM synthesis. C.M.: Development of SMPU fibers, thermal analysis (DSC, TGA). X.M.: Optimization of the process for SMPU fibers development. K.V.: Development of SMPU fibers (pristine and loaded with MEPCMs). J.L.: Thermal camera measurements and analysis. E.A.: Review and funding acquisition. M.B.: Conceptualization, writing and review. J.L.V–V.: Conceptualization, Project administration, Funding acquisition.

Declaration of competing interest

The authors declare that they have no known competing financial interests or personal relationships that could have appeared to influence the work reported in this paper.

Data availability

Data will be made available on request.

Acknowledgments

Authors would like to acknowledge the Basque Government funding within the ELKARTEK 2019 (KK-2019/00039) and ELKARTEK 2021 (KK-2021/00040) and FRONTIERS IV Prog rammes.

Appendix A. Supplementary data

Supplementary data to this article can be found online at https://doi.org/10.1016/j.polymertesting.2022.107807.

References

[1] G. Havenith, Interaction of clothing and thermoregulation, Exog. Dermatol. 1 (2002) 221–230, https://doi.org/10.1159/000068802.
[2] K. Stevens, M. Fuller, Thermoregulation and clothing comfort, in: J. McCann, D. Bryson (Eds.), Textile-Led Design for the Active Ageing Population, Woodhead Publishing, Amsterdam (Nederland), 2015, pp. 117–138.
[3] T. Ruiz-Calleja, M. Bonet-Aracil, J. Gisbert-Payá, E. Bou-Belda, Analysis of the influence of graphene and phase change microcapsules on thermal behavior of cellulosic fabrics, Mater. Today Commun. 25 (2020), 101557, https://doi.org/10.1016/j.mtcomm.2020.101557.
[4] Y. Lu, X. Xiao, Y. Liu, J. Wang, S. Qi, C. Huan, H. Liu, Y. Zhu, G. Xu, Achieving multifunctional smart textile with long afterglow and thermo-regulation via coaxial electrospinning, J. Alloys Compd. 812 (2020), 152144, https://doi.org/10.1016/j.jallcom.2019.152144.
[5] G.G.D. Han, H. Li, J.C. Grossman, Optically-controlled long-term storage and release of thermal energy in phase-change materialsm, Nat. Commun. 8 (2017) 1446, https://doi.org/10.1038/s41467-017-01608-y.
[6] Y. Cui, H. Gong, Y. Wang, D. Li, H. Bai, A thermally insulating textile inspired by polar bear hair, Adv. Mater. 30 (2018), 1706807, https://doi.org/10.1002/adma.201706807.
[7] C. Prisacariu, Chemistry of polyurethane elastomers, in: C. Prisacariu (Ed.), Polyurethane Elastomers. From Morphology to Mechanical Aspects, Springer-Verlag, Vienna (Austria), 2011, pp. 1–22.
[8] N. Adam, G. Avar, H. Blankenheim, W. Friederichs, M. Giersig, E. Weigand, M. Halfmann, F.W. Wittbecker, D.R. Larimer, U. Maier, S. Meyer-Ahrens, K. L. Noble, H.G. Wussow, Polyurethanes, in: F. Ullmann (Ed.), Ullmann's Encyclopedia of Industrial Chemistry, Wiley-VCH Verlag GmbH & Co. KGaA, Weinheim (Germany), 2012, pp. 545–604.
[9] A. Lendlein, S. Kelch, Shape-memory polymers, Angew. Chem. Int. Ed. 41 (2002) 2034–2057, https://doi.org/10.1002/1521-3773(20020617)41:12<2034::AID-ANIE2034>3.0.CO;2-M.
[10] C. Liu, H. Qin, P.T. Mather, Review of progress in shape-memory polymers, J. Mater. Chem. 17 (2007) 1543–1558. https://doi:10.1039/b615954k.
[11] M. Behl, J. Zotzmann, A. Lendlein, Shape-memory polymers and Shape -changing polymers, in: A. Lendlein (Ed.), Shape Memory Polymers. Advances in Polymer Science, Springer-Verlag, Heidelberg (Germany), 2010, pp. 1–40.
[12] W.M. Huang, Z. Ding, C. Wang, J. Wei, Y. Zhao, H. Purnawali, Shape memory materials, Mater. Today 13 (2010) 54–61, https://doi.org/10.1016/S1369-7021(10)70128-0.
[13] M. Sáenz-Pérez, E. Lizundia, J.M. Laza, J. García-Barrasa, L.M. León, J.L. Vilas, Methylene diphenyl diisocyanate (MDI) and toluene diisocyanate (TDI) based polyurethanes: thermal, shape-memory and mechanical behavior, RSC Adv. 6 (2016) 69094–69102. https://DOI:10.1039/C6RA13492K.
[14] M. Sáenz-Pérez, J.M. Laza, J. García-Barrasa, J.L. Vilas, L.M. León, Influence of the soft segment nature on the thermo-mechanical behavior of shape memory polyurethanes, Polym. Eng. Sci. 58 (2018) 238–244, https://doi.org/10.1002/pen.24567.
[15] J.M. Laza, A. Veloso, J.L. Vilas, Tailoring new bisphenol an ethoxylated shape memory polyurethanes, J. Appl. Polym. Sci. 138 (2021) 49660–49670, https://doi.org/10.1002/app.49660.
[16] F. Li, X. Zhang, J. Hou, M. Xu, X. Luo, D. Ma, B. K Kim, Studies on thermally stimulated shape memory effect of segmented polyurethanes, J. Appl. Polym. Sci. 64 (1997) 1511–1516, https://doi.org/10.1002/(SICI)1097-4628(19970523)64:8<1511::AID-APP8>3.0.CO;2-K.
[17] F. Li, J. Hou, W. Zhu, X. Zhang, M. Xu, X. Luo, D. Ma, B.K. Kim, Crystallinity and morphology of segmented polyurethanes with different soft-segment length, J. Appl. Polym. Sci. 62 (1996) 631–638, https://doi.org/10.1002/(SICI)1097-4628(19961024)62:4<631::AID-APP6>3.0.CO;2-U.
[18] B. Yang, W.M. Huang, C. Li, J.H. Chor, Effects of moisture on the glass transition temperature of polyurethane shape memory polymer filled with nano-carbon powder, Eur. Polym. J. 41 (2005) 1123–1128, https://doi.org/10.1016/j.eurpolymj.2004.11.029.
[19] B. Yang, W.M. Huang, C. Li, L. Li, Effects of moisture on the thermomechanical properties of a polyurethane shape memory polymer, Polymer 47 (2006) 1348–1356, https://doi.org/10.1016/j.polymer.2005.12.051.
[20] S. Chen, J. Hu, Y. Liu, H. Liem, Y. Zhu, Q. Meng, Effect of molecular weight on shape memory behavior in polyurethane films, Polym. Int. 56 (2007) 1128–1134, https://doi.org/10.1002/pi.2248.
[21] S. Chen, H. Yuan, Z. Ge, S. Chen, H. Zhuo, J. Liu, Insights into liquid-crystalline shape-memory polyurethane composites based on an amorphous reversible phase and hexadecyloxybenzoic acid, J. Mater. Chem. C 2 (2014) 1041–1049. https://DOI:10.1039/C3TC31612B.
[22] T. Zhao, R. Yu, X. Li, B. Cheng, Y. Zhang, X. Yang, X. Zhao, Y. Zhao, W. Huang, 4D printing of shape memory polyurethane via stereolithography, Eur. Polym. J. 101 (2018) 120–126, https://doi.org/10.1016/j.eurpolymj.2018.02.021.
[23] Y. Ji, M. Schaerlaekens, E.M. Terentjev, Innovative textile materials, stiffening procedures and fabric-joining methods, in: L.G.A. Walter Kartsounis, S. Carosio (Eds.), Transforming Clothing Production into a Demand-Driven, Knowledge-Based, High-Tech Industry, Springer, London (UK), 2009, pp. 61–93.
[24] J. Hu, H. Meng, G. Li, S.I. Ibekwe, A review of stimuli-responsive polymers for smart textile applications, Smart Mater. Struct. 21 (2012), 53001. https://doi:10.1088/0964-1726/21/5/053001.
[25] R. Meirowitz, Microencapsulation technology for coating and lamination of textiles, in: W. Smith (Ed.), Smart Textile Coatings and Laminates, Woodhead Publishing Ltd., Cambridge (USA), 2010, pp. 125–154.
[26] M. Saenz-Perez, T. Bashir, J.M. Laza, J. García-Barrasa, J.L. Vilas, M. Skrifvars, L. M. León, Novel shape-memory polyurethane fibers for textile applications, Text, Res. J. 89 (2019) 1027–1037, https://doi.org/10.1177/0040517518760756.
[27] W.D. Li, E.Y. Ding, Preparation and characterization of cross-linking PEG/MDI/PE copolymer as solid-solid phase change heat storage material, Sol. Energy Mater. Sol. Cell. 91 (2007) 764–768, https://doi.org/10.1016/j.solmat.2007.01.011.
[28] G. Alva, Y. Lin, L. Liu, G. Fang, Synthesis, characterization and applications of microencapsulated phase change materials in thermal energy storage: a review, Energy Build. 144 (2017) 276–294, https://doi.org/10.1016/j.enbuild.2017.03.063.
[29] S. Mondal, Phase change materials for smart textiles - an overview, Appl. Therm. Eng. 28 (2008) 1536–1550. https://doi:10.1016/j.applthermaleng.2007.08.009.
[30] P. Bajaj, Thermally sensitive materials, in: X.M. Tao (Ed.), Smart Fibres, Fabrics, and Clothing, Woodhead Publishing, Cambridge (USA), 2001, pp. 58–82.
[31] A. Reizabal, J.M. Laza, J.M. Cuevas, L.M. León, J.L. Vilas, PCO-LLDPE thermoresponsive shape memory blends. Towards a new generation of breathable and waterproof smart membranes, Eur. Polym. J. 119 (2019) 469–476, https://doi.org/10.1016/j.eurpolymj.2019.08.013.
[32] ASTM E 96-95 Standard Test Methods for Water Vapor Transmission of Materials, https://www.astm.org/e0096-95.html (archived on 23-02-2022.
[33] Z. Song, H. Xiao, Y. Zhao, Hydrophobic-modified nano-cellulose fiber/PLA biodegradable composites for lowering water vapor transmission rate (WVTR) of paper, Carbohydr. Polym. 111 (2014) 442–448. https://DOI:10.1016/j.carbpol.2014.04.049.
[34] E. Bugnicourt, P. Cinelli, A. Lazzeri, V. Alvarez, Polyhydroxyalkanoate (PHA): review of synthesis, characteristics, processing and potential applications in packaging, Express Polym. Lett. 8 (2014) 791–808. https://DOI:10.3144/expresspolymlett.2014.82.
[35] R. Wilson, S.C. George, A. Kumar, S. Thomas, Liquid transport characteristics in polymeric systems: an introduction, in: S. Thomas, R. Wilson, A. Kumar, S. C. George (Eds.), Transport Properties of Polymeric Membranes, Elsevier, Amsterdam (Netherlands), 2018, pp. 3–13.
[36] A. Mukhopadhyay, V.K. Midha, A review on designing the waterproof breathable fabrics Part I: fundamental principles and designing aspects of breathable fabrics, J. Ind. Textil. 37 (2008) 225–262, https://doi.org/10.1177/1528083707082164.
[37] S. Zekriardehani, S.A. Jabarin, D.R. Gidley, M.R. Coleman, Effect of chain dynamics, crystallinity, and free volume on the barrier properties of poly(ethylene terephthalate) biaxially oriented films, Macromolecules 50 (2017) 2845–2855, https://doi.org/10.1021/acs.macromol.7b00198.
[38] W. Xie, H. Ju, G.M. Geise, B.D. Freeman, J.I. Mardel, A.J. Hill, J.E. McGrath, Effect of free volume on water and salt transport properties in directly copolymerized disulfonated poly(arylene ether sulfone) random copolymers, Macromolecules 44 (2011) 4428–4438, https://doi.org/10.1021/ma102745s.
[39] E. Axpe, N. García-Huete, J.M. Cuevas, C. Ribeiro, D. Mérida, J.M. Laza, J. A. García, J.L. Vilas, S. Lanceros-Méndez, F. Plazaola, L.M. León, Connecting free volume with shape memory properties in non-cytotoxic gamma irradiated polycyclooctene, J. Polym. Sci., Part B: Polym. Phys. 53 (2015) 1080–1088, https://doi.org/10.1002/polb.23750.
[40] N. García-Huete, E. Axpe, J.M. Cuevas, D. Mérida, J.M. Laza, J.A. García, J.L. Vilas, F. Plazaola, L.M. León, In situ measurements of free volume during recovery process of a shape memory polymer, Polymer 109 (2017) 66–70, https://doi.org/10.1016/j.polymer.2016.12.042.
[41] S. Kasapis, I.M. Al-Marhoobi, J.R. Mitchell, Testing the validity of comparisons between the rheological and the calorimetric glass transition temperature, Carbohydr. Res. 338 (2003) 787–794. https://DOI:10.1016/s0008-6215(03)00012-0.
[42] J. Kaursoin, A.K. Agrawal, Melt spun thermoresponsive shape memory fibers based on polyurethanes: effect of drawing and heat-setting on fiber morphology and properties, J. Appl. Polym. Sci. 103 (2007) 2172–2182, https://doi.org/10.1002/app.25124.
[43] X.M. Ding, J.L. Hu, X.M. Tao, C.P. Hu, Preparation of temperature sensitive polyurethanes for smart textiles, Text, Res. J. 76 (2006) 406–413, https://doi.org/10.1177/0040517506063389.
[44] J. Hu, Y. Zhu, H. Huang, J. Lu, Recent advances in shape-memory polymers: structure, mechanism, functionality, modeling and applications, Prog. Polym. Sci. 37 (2012) 1720–1763. https://DOI:10.1016/j.progpolymsci.2012.06.001.